Available online at www.sciencedirect.com
ScienceDirect
Catalysis Today 124 (2007) 61–70
CATALYSIS TODAY
www.elsevier.com/locate/cattod

Surface reaction kinetics studied with nanoscale lateral resolution

Matthieu Moors, Thierry Visart de Bocarmé, Norbert Kruse *

Chemical Physics of Materials, Université Libre de Bruxelles, Campus de la Plaine, CP 243, B-1050 Bruxelles, Belgium

Available online 23 March 2007

Abstract

This paper reviews some of the recent progress made in local probing of catalytic and non-catalytic surface reactions using relaxation-type pulsed field desorption mass spectrometry (PFDMS) in combination with video-field ion microscopy (FIM). First, the carbonylation of nickel to $Ni(CO)_4$ is shown to involve surface Ni subcarbonyls as intermediates. Time-resolved PFDMS studies reveal $Ni(CO)_2$ formation to be the slowest step in the overall reaction. Based on repetitive $Ni(CO)_2$ formation in kink sites, a model is presented to explain morphological reshaping of Ni 3D field emitter crystals as observed previously by FIM. Second, we show that Co subcarbonyls, $Co(CO)_{2,3}$, are formed during the interaction of CO and mixtures of CO/H_2 with Co 3D crystals. CO dissociation and build-up of C_xH_y species are followed in real-time. Methane is the first product of hydrogenation, longer-chain hydrocarbons are detected by field pulses under steady reaction conditions. Finally, video-FIM data are presented for the ethylene reaction with Ni 3D crystals at elevated temperatures. Subsequent treatment of the Ni specimen with hydrogen, oxygen or by applying high electric fields in the absence of these gases results in the observation of non-linear reaction phenomena which are interpreted as being due to a clean-off titration of carbon. Chemical fronts seem to ignite in (0 0 1) planes and eventually travel to the central (1 1 1) plane.

Keywords: Field ion microscopy; Atom-probe; Carbon monoxide; Ethylene; Nickel; Cobalt; Fischer-Tropsch; Catalysis

1. Introduction

Dynamic methods based on transient kinetic measurements have a long history in catalysis research and may provide information on reaction pathways under truly in situ reaction conditions, see ref. [1], for a survey of achievements. Ultimately, one would like to perform such measurements by probing the local chemical surface composition in a time-resolved manner while imaging surface atomic arrangements and active sites along with single molecules reacting with these. Unfortunately, such detailed information cannot be gleaned by any method alone so that research strategies have been developed in the past which usually consist in combining several complementing methods. Still, in many cases, materials and pressure conditions have to be adjusted to enable the application of these methods. Despite the detailed atomic-scale understanding of surface reaction processes that may be acquired from research under such idealized conditions, questions persist as to the validity of the approach and the significance for real heterogeneous catalysis.

More recent developments in transmission electron microscopy (TEM) have allowed atomic-scale imaging of supported metal nanoparticles and their shape transformations under reactive atmospheres [2,3]. The combination of high spatial resolution in TEM with local electronic properties as measured by electron energy loss spectroscopy (EELS) may be regarded as particularly attractive [4] but must probably await further technical refinements for its use to full capacity. Scanning tunnelling microscopy (STM) and atomic force microscopy (AFM), see refs. [5,6] for recent reviews, have come a long way to provide unprecedented structural information of surfaces under variable environmental conditions, however, an easy access to chemical mapping of surface species with unknown composition turns out to be difficult, if not impossible with these techniques.

With this background atom-probe field ion/desorption mass spectrometry remains an attractive alternative in basic catalysis research, with the restriction that samples have to be conducting and available in form of tips. Such tips are nearly hemispherical and can be imaged with atomic resolution using field ion microscopy (FIM) (for a review

* Corresponding author.
E-mail address: nkruse@ulb.ac.be (N. Kruse).

0920-5861/$ – see front matter © 2007 Elsevier B.V. All rights reserved.
doi:10.1016/j.cattod.2007.01.063

of the basic principles, see ref. [7]). More recent developments have demonstrated video-FIM to be a valuable tool for imaging catalytic surface reactions [8] and making visible morphological shape transformations with nanoscale lateral resolution [9]. For a recent review of achievements, see ref. [10]. Since a field emitter tip may be regarded as an excellent model of a ''single catalyst grain'' in the absence of a ceramic support, most detailed information on the role of edges and kinks as active sites in catalysis can be obtained. Moreover, atomic-scale resolution in FIM can be directly combined with local chemical probing in pulsed field desorption mass spectrometry (PFDMS). The latter is basically a relaxation-type technique in which short field pulses of variable repetition frequency are applied to remove adsorbed species during the ongoing reaction and to analyse respective ions in a mass spectrometer. Several case studies will be presented in this paper. First, the non-catalytic formation of $Ni(CO)_4$ from Ni and CO is inspected before a more complicated example of catalysis research is addressed: the catalytic hydrogenation of CO on Co. We end by presenting first FIM results on the reaction with oxygen of a Ni surface subjected to ethylene adsorption and decomposition.

2. Experimental

2.1. General

The first PFDMS set-up was described as early as in 1975 [11]. The basic principles are still the same in more recent instrumentation. A full account of the systems characteristics at the ULB will be provided elsewhere. Fig. 1 assembles: (i) a field ion micrograph of a Ni tip (a) along with a ball model to demonstrate the 3D specimen morphology (b) and (ii) a scheme illustrating atom-probe PFDMS measurements (c) along with field desorption using pulses (d).

To summarize the PFDMS operational principles, short field pulses of some 100 ns are used to field desorb adsorbed species during the ongoing catalytic reaction, i.e. while running the instrument as a flow reactor at overall low steady gas pressures ($p \leq 2 \times 10^{-2}$ Pa). Respective ions are injected via a small probe-hole into a time-of-flight mass spectrometer. The probe-hole usually selects between 100 and 400 atomic sites of a field emitter tip. An electrostatic lens inside the flight tube can be optionally used to adjust the size of the monitored area. Tilting the tip in front of the probe hole allows different crystallographic planes to be investigated for their chemical reactivity.

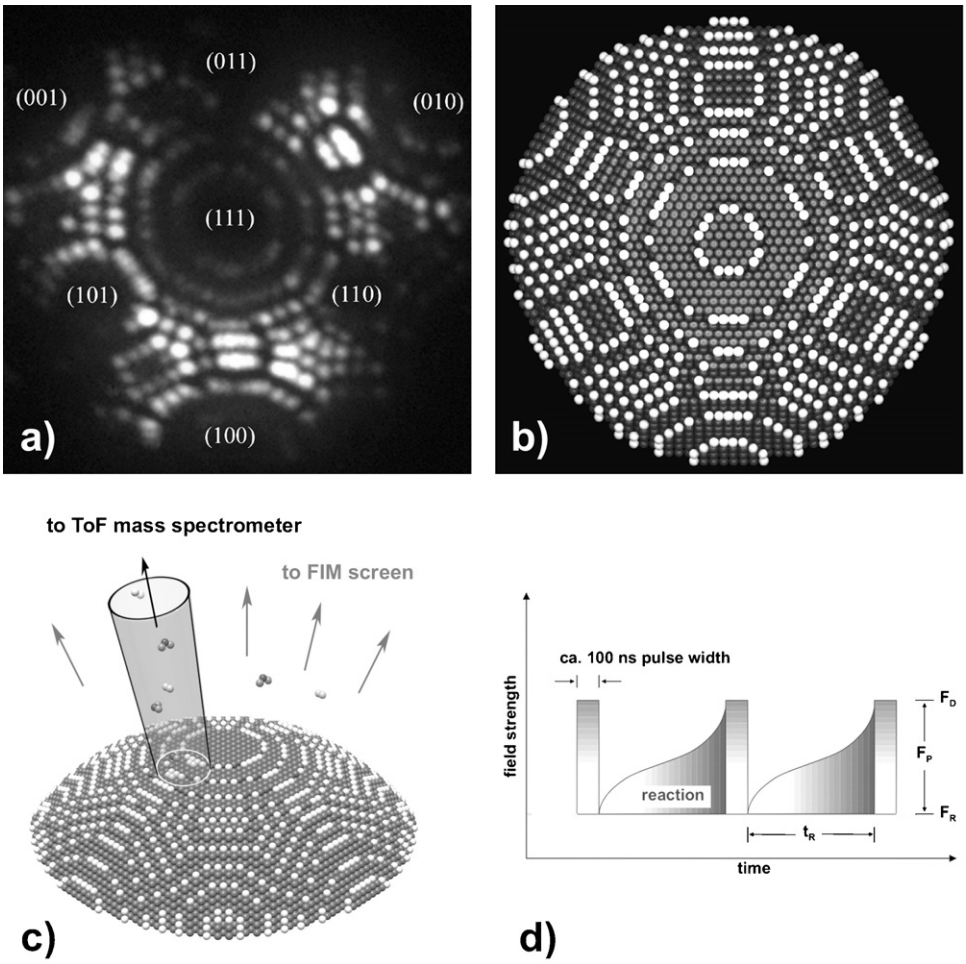

Fig. 1. Field ion micrograph of a [1 1 1] oriented Ni tip (a) along with a ball model (b), scheme of the atom-probe technique for a [0 0 1] oriented ball model (c) and field desorption by pulses of defined repetition frequency (d).

Field ion micrographs can be recorded during chemical probing. For this purpose, a mirror (containing a central hole for ion passage) is mounted at the rear of a channel plate image intensifier and rotated by 45° about the vertical axis.

Field emitter tips are electrochemically etched from thin metal wires ($\phi \sim 0.1$ mm). Specimens of Co are prepared in $CH_3COOH/HClO_4$ (20:1) those of Ni in diluted HCl (0.5 mol/l). Tip radii of curvature are between ~10 (or even less) and 50 nm depending on the actual etching procedure. Tips are characterized by field ion microscopy (FIM). Cycles of thermal annealing, Ne^+ or Ar^+ sputtering and field evaporation are used to clean the tips before using them in reaction studies.

2.2. Kinetic measurements [12]

Field pulses ($F < 40$ V/nm, widths ~100 ns) serve two purposes: (i) they cause field desorption of the adsorbed layer after a reaction time provided by the repetition frequency (≤100 kHz) of the pulses and (ii) they define a new reaction time period with starting conditions varying between zero and steady-state coverage, corresponding to field desorption with complete and, respectively, negligible layer removal. Quantification can only be achieved if field pulses cause complete desorption of the adsorbed layer. In that case, ion intensities reflect surface coverages and the latter can be calculated provided the size of the monitored surface area is known.

Qualitative insight into the surface layer composition is obtained by using low-amplitude field pulses. Under these conditions, the layer composition is nearly constant throughout the measurements; small amounts removed by pulses are immediately refilled by adsorption between pulses. The identification of true surface species is not straightforward under these conditions unless patterns of species' fragmentation or association are known. Quite generally, assignments can be facilitated through temperature and pressure variation. However, the PFDMS method also allows to study the influence of the electric field strength through independent variation of the field pulse amplitude and the dc field. This procedure has been recently applied to reveal the field-promoted carbonyl formation on gold surfaces.

In Fig. 1d, the general experimental procedure for kinetic measurements is illustrated for field pulse amplitudes high enough to cause quantitative desorption. Adsorption takes place during t_R, while gaseous reactants impinge onto the surface. A dc field may be applied arbitrarily. The field pulses stop the adsorption process and cause desorption of the adsorbed layer.

Kinetic data of surface reactions can be obtained by varying the repetition rate, i.e. the reaction time t_R between the field pulses. This is usually done by scanning the time range from 100 μs up to some seconds. Three different pulse repetition rates, corresponding to short, medium, and long field-free times, t_R, are depicted in Fig. 2. For short times, as indicated on the left-hand side of the figure, the surface coverage that can be reached by adsorption during t_R is far below the monolayer limit. Only the initial stages of adsorption are monitored under these conditions. At medium t_R, field pulses will detect intermediate species while at long times the surface reaction

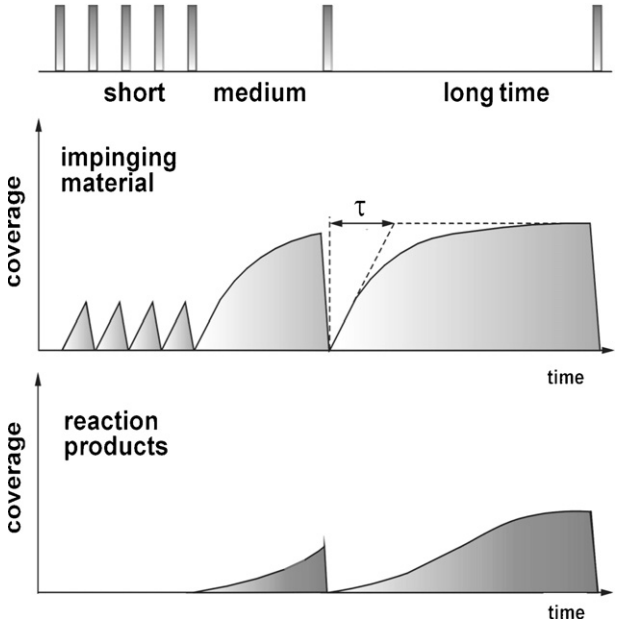

Fig. 2. Evaluation of kinetic data from pulsed field desorption measurements: (top) time scheme of pulses; (bottom) development of surface concentrations for impinging material and reaction products; relaxation times τ for processes in the adsorbed layer can be determined from measurements with variable pulse repetition frequencies (reaction times).

may run into a steady state so that the probability of product formation increases. Alternatively, depending on temperature and pressure, the surface coverage may also reach saturation. In fact, severe site blocking may occur if the partial pressures of reactants are not properly adjusted. Such a case will be demonstrated later for the CO hydrogenation on Co model catalysts.

3. Results and discussion

3.1. Formation of $Ni(CO)_x$ during the reaction of CO with Ni

The chemisorption of carbon monoxide on nickel surfaces is one of the most frequently studied gas/solid systems in surface science. Less work, however, was devoted to the dissolution process [13–23], $Ni_s + 4CO_g \Leftrightarrow Ni(CO)_{4,g}$, which has a long-standing history associated with the *Mond* process [24] of Ni manufacture and refinery. Indeed, from the viewpoint of equilibrium thermodynamics ($K_p = 7.2 \times 10^3$ bar^{-3} corresponding to a standard free energy, $\Delta G_R{}^0 = -22.6$ kJ/mol), complete carbonylation should not occur at low pressures, say $p_{CO} < 1$ Pa. PFDMS work in the early eighties yet demonstrated that Ni-subcarbonyl species, $Ni(CO)_x$ ($x = 1$–3), can be formed at $p_{CO} = 10^{-4}$ Pa in the presence of a dense (''compressed'') CO overlayer structure on a Ni field emitter surface [25,26]. Fig. 3 shows a respective time-of-flight mass spectrum obtained by probing the stepped surface region close to the Ni(0 0 1) pole of the emitter tip during its interaction with CO gas at 5×10^{-3} Pa at 300 K. Clearly, there are Ni^+ and Ni^{2+}, both originating from field evaporation, as well as CO^+

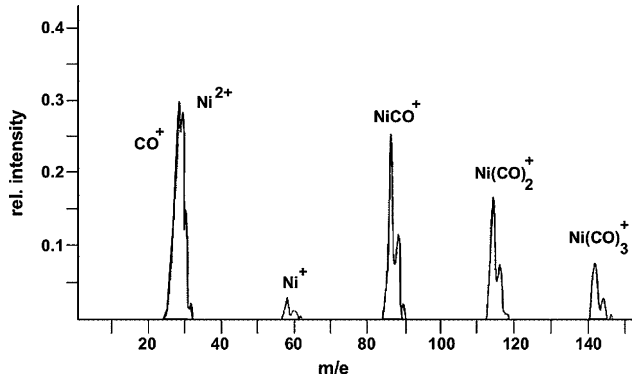

Fig. 3. Typical time-of-flight mass spectrum obtained by probing a region close to the Ni(0 0 1) pole of the emitter tip; $Ni(CO)_4^+$ is absent due to immediate thermal desorption of the neutral molecule; $p_{CO} = 2 \times 10^{-3}$ Pa, $T = 300$ K.

and $Ni(CO)_x^+$ species resulting from the adsorption and reaction of CO. Most remarkably, $Ni(CO)_4^+$ species are missing in the spectrum. This was formerly interpreted as being due to the non-occurrence of the final stage in the carbonylation sequence [26]. More recently, however, we proved that $Ni(CO)_4$ species yet are formed. The proof was based on the titration by Auger electron spectroscopy (AES) of Ni deposits on an auxiliary surface (Rh in this case) after $Ni(CO)_4$ vaporization from a Ni foil which was first sputter-roughend and subsequently exposed to low pressures of CO gas [27]. With regard to Fig. 3, it must be concluded that $Ni(CO)_4$ undergoes fast thermal desorption thus escaping detection by field pulses. A mean life time $\tau \approx 6 \times 10^{-7}$ s (assuming a pre-exponential $\tau_0 \approx 10^{-13}$ s) at 300 K can be estimated from studies of $Ni(CO)_4$ adsorption on Ni [28]. As will be shown below, this time is much shorter than the characteristic times measured for Ni-subcarbonyl formation.

The desorption field strength used for the measurements leading to Fig. 3 amounts to ~21 V/nm. It was previously shown [25] that while chemisorbed CO is not completely removed (as CO^+ and $Ni(CO)^+$) by pulses producing this field strength, adsorbed Ni-subcarbonyls, $Ni(CO)_x$, yet are. In fact, this is a prerequisite for kinetic studies and allows to convert measured ion intensities into surface coverages.

Fig. 4 presents results obtained from reaction time variation. Obviously, the chemisorbed layer reaches saturation after a reaction time of ~1 ms at a CO pressure of 3×10^{-4} Pa. This short time reflects the fast refilling of the CO_{ad} layer after desorption of only small amounts at a field strength of 20.6 V/nm (pulses only, no steady field present). $Ni(CO)_2$ and $Ni(CO)_3$ build up in measurable amounts after saturation of the chemisorbed layer at $t_R \sim 1$ ms. Experiments at higher field strengths were found to shift both, the characteristic time for refilling the chemisorbed layer as well as the induction period for Ni-subcarbonyl formation. Thus, saturation of the CO_{ad} layer is a prerequisite for Ni-subcarbonyl formation. Low energy electron diffraction (LEED) on Ni(1 0 0) [29] has demonstrated that a compressed overlayer structure is formed under saturation conditions. The low binding energy of CO_{ad} in such a structure seems to play an important role in the energetics of Ni-carbonyl formation.

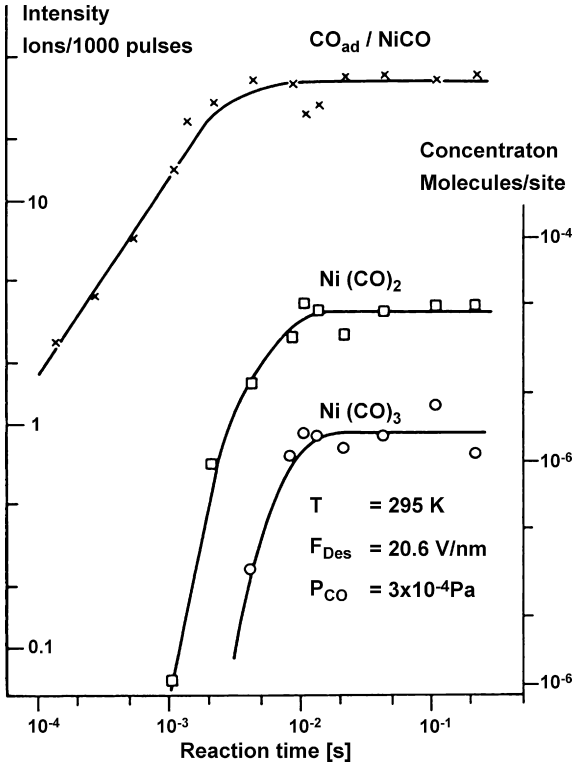

Fig. 4. PFDMS results obtained by varying the reaction time t_R at $p_{CO} = 3 \times 10^{-4}$ Pa, 300 K and $F_D = 20.6$ V/nm; Ni-subcarbonyl intensities are converted into surface coverages; monitored area 9.5 nm^2, containing 150 surface sites; impingement rate: 450 CO molecules/s.

The initial slopes of $Ni(CO)_{2,3}$ formation indicate that a reaction process is in operation which is more strongly dependent on the reaction time than is CO chemisorption. This is in accordance with a consecutive surface reaction involving the successive addition of two and, respectively, three CO molecules to a single Ni atom with the latter being most likely in a kink site position. The initial rate of formation is of the order of 10^{-2} $Ni(CO)_2$ molecules/sites.

Both $Ni(CO)_2$ and $Ni(CO)_3$ reach constant coverages after a (pseudo) first order relaxation time of $\tau_1 \sim 10$ ms which is about one order of magnitude longer than the respective time $\tau_2 \sim 1$ ms for refilling the CO_{ad} layer up to the $(1 - 1/e)$ level of saturation. Thus, the rate determining step of carbonylation is associated with $Ni(CO)_2$ formation.

Constant Ni-subcarbonyl coverages at long reaction times reflect steady state conditions, i.e. Bodenstein's principle applies and the rates of forward reactions equal those of backward reactions. The final product, $Ni(CO)_4$, does not appear in measurable quantities in Fig. 4. Once being formed, this species undergoes thermal desorption, with no chance of being readsorbed on the Ni tip surface.

Based on the above experimental evidence, a reaction mechanism was proposed of which the essential features are schematically summarized in the ball model of Fig. 5. Accordingly, CO adsorption is envisaged to take place at terraces and steps (for the sake of clarity only a few CO_{ad} molecules are considered in an otherwise saturated overlayer

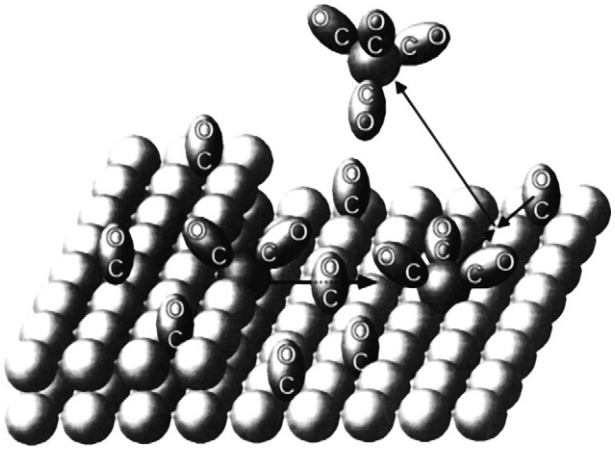

Fig. 5. Model of $Ni(CO)_4$ formation starting at a kink-site; for reasons of clearness only a few CO molecules of the compressed adlayer are shown.

structure). Ni-dicarbonyl formation is the result obtained by adding a terrace-site CO_{ad} to an occupied lowest-coordination step site (kink). The reaction

$$Ni(CO)_{kink} + CO_{ad} \underset{k_{-2}}{\overset{k_2}{<=>}} Ni(CO)_{2,ad} + \square_{kink}$$

is associated with Ni–Ni bond breaking in kink sites. Once $Ni(CO)_{2,ad}$ is liberated, it rapidly reacts to form $Ni(CO)_{3,ad}$ and, finally, $Ni(CO)_4$ which undergoes immediate thermal desorption.

The liberation of a $Ni(CO)_{2,ad}$ species usually reproduces a kink site, i.e. the above reaction step occurs repetitively until either an open chain of Ni atoms is used up or inhibition comes into play as, for example, by carbon deposition due to CO_{kink} decomposition. Clearly, this reaction mechanism must lead to structural changes of the surface. According to observations by Schmidt et al. [23], kink sites of a Ni tip surface are indeed annihilated during the reaction with CO. In particular, the hemispherical Ni tip surface was found to develop low-index planes of a polyhedron.

The results described above demonstrate the full power of the PFDMS technique in determining mechanisms and quantifying kinetic processes in adsorbed layers with a lateral resolution on the nanoscale. The occurrence of high step densities is one of the characteristic features of 3D field emitter tips. Both morphology and topography of such specimens are thermodynamically not in equilibrium. This must be carefully considered in analyzing PFDMS data. The effect is most strikingly manifested by the studies presented above: at a CO pressure of 3×10^{-4} Pa a carbonylation rate of $\sim 10^{-2}$/site's is determined from the slope of Fig. 4 on a *non-equilibrium* Ni surface whereas a *maximum* rate of only 3.4×10^{-23}/site's would be calculated for the same pressure on an *equilibrium* surface (note that under equilibrium conditions the rates of $Ni(CO)_4$ formation and decomposition are equal and that the maximum decomposition rate is given by the impingement rate of $Ni(CO)_4$ at its equilibrium pressure). From a more general point of view of heterogeneous catalysis, the above results predict that supported Ni catalyst particles always suffer redispersion in the presence of CO gas. Ultimately, Ni may be removed from the catalytic reactor through $Ni(CO)_4$ gas phase transport. The empirical criterion for stable particle sizes defined by Shen et al. [22] according to which the equilibrium pressure $p(Ni(CO)_4) < 10^{-8}$ mbar corresponding to $p_{CO} \sim 0.1$–1 bar, is misleading because it does not take into account the morphology of the Ni catalyst. Furthermore, this criterion is based on thermodynamic properties which do not properly describe the rather complicated reaction far from equilibrium.

The phenomenon of subcarbonyl formation on stepped (non-equilibrium) surfaces seems to be of quite general importance. PFDMS studies with Co, Ru, Rh and Pd field emitter tips gave clear evidence for the formation of mobile $Me(CO)_{x,ad}$ (x up to 4 for Ru). The Co case will be inspected below in context with CO hydrogenation.

3.2. CO adsorption and hydrogenation on Co

Fears for limited supply of crude oil in a globalizing world have spurred the search for alternative fuel provisions. The ''gas-to-liquid'' technology via the Fischer Tropsch synthesis (FTS) stands out as most promising in this respect. Despite being considered as a proven technology many aspects of more fundamental character remain poorly understood at present. Quite strikingly, Co, Fe and Ru based catalysts may be employed but no universally valid reaction mechanism seems to be available for either catalyst. An overview of the complexity of FTS in general and the various proposed mechanisms in particular, can be found in ref. [30].

In this contribution, we shall raise the question for the layer chemical composition on Co 3D tips and for the kinetics of species' formation during gas adsorption. We first turn to CO adsorption which has been studied by dosing a [1 0 0] oriented tip at a steady pressure of 1.3×10^{-2} Pa and 450 K. Using the probe hole technique ~200 atomic sites of the (0 0 0 1) plane are monitored by field pulses of an amplitude close to 30 V/nm. Under these conditions, complete field desorption of the adsorbed layer is achieved so that the species' intensities reflect surface coverages. Separate experiments with varying field strengths (not shown here) have indeed demonstrated that complete layer desorption by pulses is achieved at field strengths above 28 V/nm. Under these conditions, considerable amounts of field evaporated Co^+ and Co^{2+} species appear in the time-of-flight mass spectra.

The mass spectra acquired under the above conditions contain a variety of different species. Quite generally we can distinguish between molecular, associative and dissociative CO adsorption. CO^+ and $CoCO^+$ species are considered representative of molecular CO adsorption. For energetic reasons of ion formation, $CoCO^+$ most probably involves step and kink sites, i.e. these species are representative of step-bound CO. Co-subcarbonyls, $Co(CO)_x^+$ (x = 2, 3) indicate associative adsorption. Obviously, similar to the Ni case discussed in length in the foregoing section, part of the chemisorbed CO forms ''twins or triplets''. Again, for energetic (but also for steric) reasons such

multiple bound CO most probably involves Co step and kink atoms. Finally, the occurrence of C^{2+}, C^+, C_2^+ and O^+ demonstrates CO dissociation to take place as well. Surface carbon and oxygen may also be field desorbed as Co_2O^{2+}, CoO^+, CoC^+ and CoC_2^+. Usually, the higher the field strength the more these species dominate over the Co-free analogues.

In Fig. 6, the ion intensities are plotted as a function of the reaction time under field conditions leading to quantitative desorption. It is seen that the surface coverage of chemisorbed CO (the sum of CO^+ and $CoCO^+$) increases linearly with time. Thus, CO adsorption at low coverages follows usual Langmuir kinetics with a constant sticking probability. Associative CO adsorption leads to $Co(CO)_2$ formation. The ion intensities are quite low (they are even lower for $Co(CO)_3^+$ which are not included here) and subject to large statistical fluctuations; a kinetic analysis similar to the Ni case cannot be provided here. Note that a major difference between Co and Ni subcarbonyls seems to be the range of CO coverages necessary for their formation. While for Ni a dense (''compressed'') CO adlayer is a prerequisite for $Ni(CO)_{2,3}$ formation no such constraint is found for Co.

Particular interest concerns the build-up of ''carbidic and oxidic phases''. According to Fig. 6 (the sum of Co_2O^{2+}, CoO^+ and of C^{2+}, C^+, C_2^+, CoC^+, CoC_2^+ intensities are represented), a process of higher kinetic order, $d\ln(\theta)/d\ln t_R \sim 2$, is in operation. In fact, this finding is in agreement with a consecutive reaction model in which molecular CO adsorption occurs first and dissociation successively. It might be suspected that CO dissociation and subcarbonyl formation are competitive processes: both are likely to involve steps and kinks. At 450 K, the dissociation process seems to dominate and we suggest that this is the reason for the relatively low $Co(CO)_x$ intensities. Note that carbonylation on Ni was studied at 300 K so that the dissociation was much less important there. Long-time exposure to CO yet may cause considerable site blocking effects on Ni as shown in studies with sputter-roughened Ni foils [27].

Surface coverages in Fig. 6 remain low. Assuming high CO sticking probabilities—a value of 0.9 was reported for the Co(0 0 0 1) surface [31] the highest values reached are of about 1% of a monolayer. Thus, our Co model catalyst remains in a ''metallic'' state within the range of measured reaction times. If an extrapolation is made to $t_R \geq 20$ ms, we expect the surface coverages of carbon and oxygen to be similar to those of molecular CO at $t_R \sim 0.2$ s. It is most probable that while further increasing t_R: (i) the CO sticking probability decreases and (ii) oxidic and carbidic species likely dominate the catalytically active phase under steady reaction conditions.

We next discuss PFDMS data on the early stages of hydrocarbon formation while dosing the Co tip with a mixture of CO and hydrogen. Fig. 7 compares respective time-of-flight mass spectra obtained at a reaction time of 1 ms (top) and 1 s (bottom) at otherwise constant reaction conditions: $p_{tot} = 10^{-1}$ Pa, $p_{H_2}/p_{CO} = 2$, $T = 500$ K. Again, the field strength has been adjusted such that quantitative field desorption is achieved. Large quantities of Co^+ and Co^{2+}

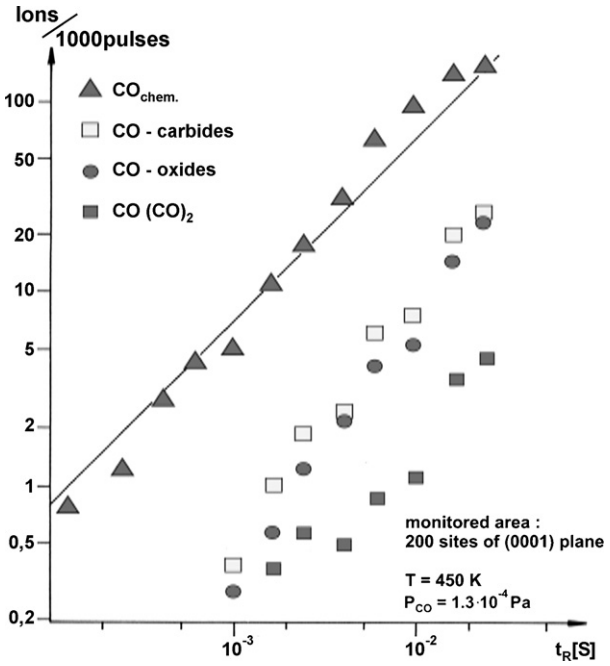

Fig. 6. Time-dependence of ion intensities detected during CO reaction with a Co tip (the model catalyst) at 450 K, $p_{CO} = 1.3 \times 10^{-3}$ Pa and ~30 V/nm. No steady electric field is applied.

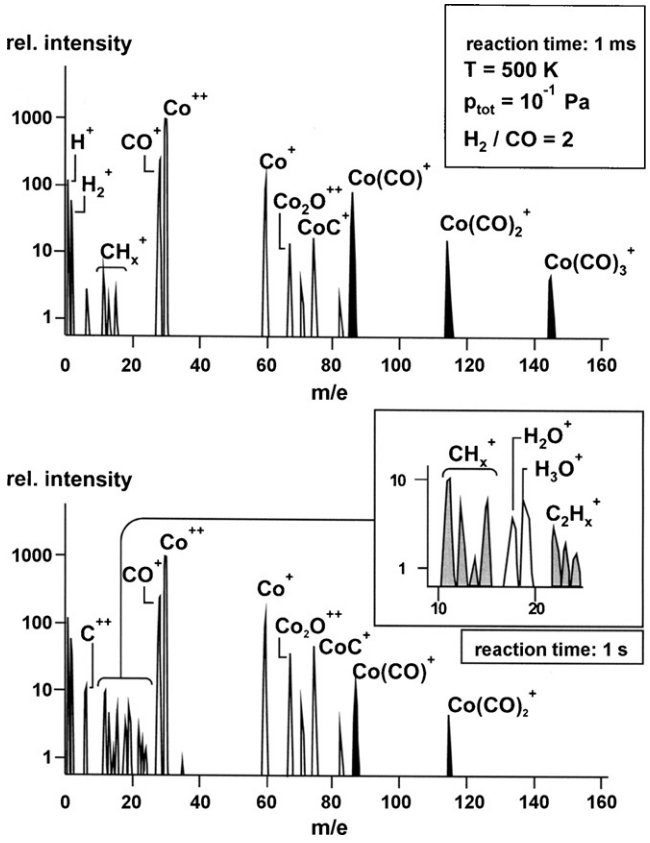

Fig. 7. Relative ion intensities during CO hydrogenation on Co at short time $t_R = 1$ ms and long time $t_R = 1$ s. Experimental conditions as indicated in the inset. The field strength is high (close to 30 V/nm) to ensure quantitative desorption and kinetic conditions without inhibition effects.

(the most abundant species with absolute numbers of several thousand ions in each spectrum) are formed under these conditions. As to be expected, considerable amounts of carbidic and oxidic species build up during the field-free (no dc field) reaction times. Particular interest concerns the occurrence of ionic CH_x species the neutrals of which can be considered reactive intermediates of the methanation reaction. The occurrence of C^+, CH^+ and CH_2^+ in the top spectrum indicates surface carbon to react with hydrogen in a stepwise manner to $CH_{2,ad}$ during $t_R = 1$ ms. Increasing the reaction time to 1 s (bottom spectrum) probably leads to methane production. This is indicated by the additional appearance of CH_3^+ species in the respective mass spectrum. The reaction product, CH_4, undergoes thermal desorption and thus escapes detection by field pulses. The concomitant formation of water which is desorbed as H_2O^+ or H_3O^+, may be considered another indication that methane forms under reaction conditions chosen in the experiment. We mention that relaxation-type studies using Chemical Transient Kinetics on either pure or supported Co catalysts have demonstrated methane to form first and CO thermal desorption subsequently. This is in complete agreement with our PFDMS studies in which pulses have to enforce field desorption of otherwise accumulating CO and $Co(CO)_{2,3}$ surface species.

Quite interestingly, subcarbonyl species, $Co(CO)_x$, are also formed during CO hydrogenation. Such species have previously been considered to be involved in the restructuring of Co model catalysts [31,32]. Following CO hydrogenation at 0.4 MPa and 520 K on a flat Co(0 0 0 1) single crystal scanning tunnelling microscopy demonstrated roughening of the initially flat surface along with homogeneous island formation. An etch-regrowth mechanism mediated by surface transport of Co atoms, possibly in the form of carbonyls, was considered. The present PFDMS study proves that Co-subcarbonyls are indeed formed. Future studies will address the question for $Co(CO)_{x,ad}$ mobility in more detail.

We finally turn to a steady layer analysis while dosing the Co model catalyst at 405 K and $p_{tot} = 4 \times 10^{-2}$ Pa ($p_{H_2}/p_{CO} = 2$). In order to render possible this analysis, field pulses of moderate amplitude, $F_D = 25$ V/nm, have been employed. Under these conditions, field desorbed amounts are immediately refilled by adsorption between pulses. The results, shown in Fig. 8, are presented in form of a time-of-flight spectrum (in fact, several spectra with different pulse repetition frequencies have been summed up and normalized to the intensity of Co^{2+} which is the most abundant species). As compared to Fig. 7, $C_xH_y^+$ ($x = 1$–4, $y \leq 3$) rather than Co-carbides or -oxides occur. Thus, Co–C_x bonds rather than Co–CoC_x bonds are broken. Moreover, no Co-subcarbonyls, $Co(CO)_x^+$, are detected. It must be concluded that the surface composition is dominated by carbon species which accumulate with time (due to incomplete field desorption) and react partially with adsorbed hydrogen. Possibly step sites are pinned by carbon species so that Co-subcarbonyl formation is prevented. Again, as mentioned above, Co based catalysts under realistic conditions of the Fischer Tropsch synthesis are most likely not in a metallic state.

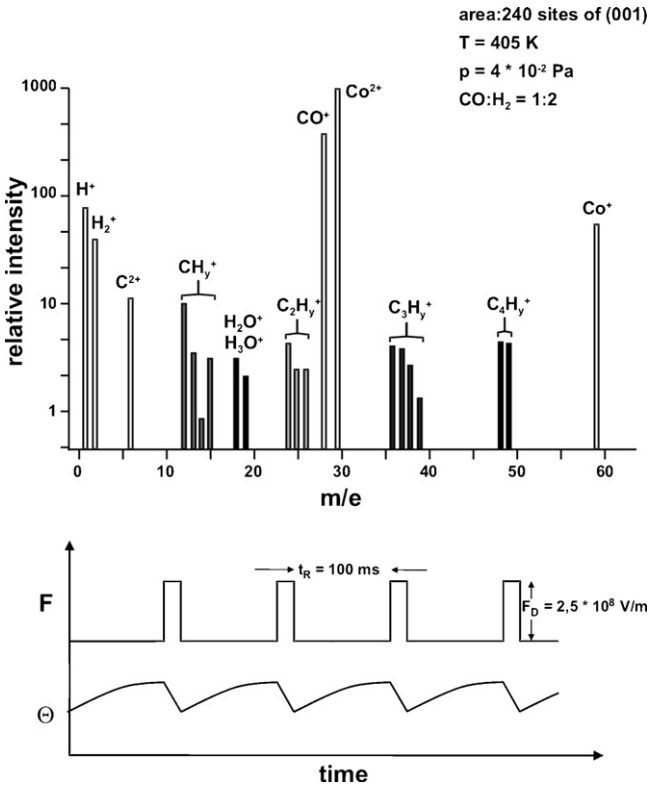

Fig. 8. Relative ion intensities during CO hydrogenation on Co at 405 K, $p = 4 \times 10^{-2}$ Pa, $CO/H_2 = 1{:}2$ and $F_D = F_P = 25$ V/nm. A mean-value spectrum is constructed from individual spectra taken under field strength conditions insufficient to ensure complete desorption.

3.3. Ethylene decomposition and reaction with oxygen on Ni

Hydrogenation and dehydrogenation reactions of simple hydrocarbons have been of considerable research interest ever since the original Nobel prize winning work of Sabatier [33]. Most recently, Vang et al. [34] have performed measurements by scanning tunnelling microscopy to demonstrate the importance of steps in the decomposition of ethylene. At a reaction temperature of 500 K, ordered islands of a ''clock''-reconstructed carbide structure have been seen to grow from the upper step edges of a Ni(1 1 1) single crystal. Ethylene decomposition then seems to continue into the terraces. Different from these observations, Nakano et al. [35] report no step nucleation of carbide at 500 K. Following ethylene adsorption at temperatures slightly higher than 600 K, ''string-like'' structures have been observed and interpreted as being due to the coalescence of isolated carbide.

In the following, we shall present video-FIM data of the carbon removal by oxygen during ethylene decomposition at 615 K on a [1 1 1] oriented Ni tip. The results are presented as a series of snapshots in Fig. 9. The starting condition just before oxygen addition is shown in Fig. 9a. The micrograph is of relatively low contrast. A few string-like patterns of up to several nm length yet appear all over the micrograph and probably indicate the occurrence of local surface reconstruction involving carbidic carbon. Adding oxygen gas to produce an

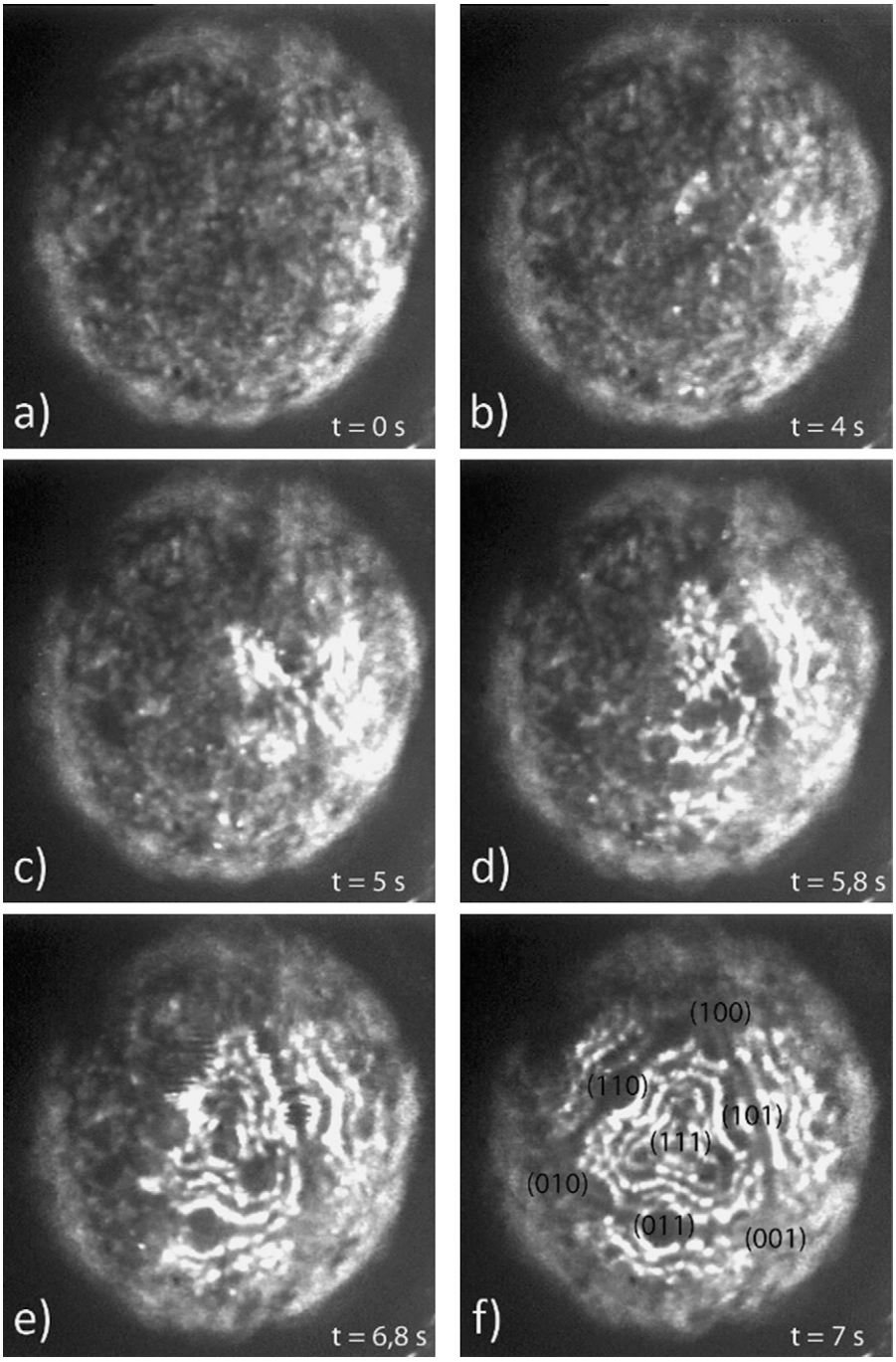

Fig. 9. Sequence of six micrographs obtained while adding oxygen gas to a Ni tip under reaction with ethylene at 615 K: (a) pure ethylene (1×10^{-3} Pa), (b–f) coadsorption and reaction of ethylene (1×10^{-3} Pa) and oxygen (2×10^{-3} Pa). The tip is kept at a constant imaging field of ~12 V/nm during the measurements. Reaction times are indicated relative to $t = 0$ of micrograph 'a'. Miller indices in micrograph 'f' serve as a guide to the eye indicating the presence of crystal planes in the final Ni tip morphology.

O_2/C_2H_4 mixture at a partial pressures ratio of 2:1 (the ethylene partial pressure of 1×10^{-3} Pa remains unchanged throughout the measurements) causes brightness changes which first appear after 4 s in the layer edges around the (1 0 1) plane. Obviously carbon atoms produced by ethylene decomposition are removed from the surface in a titration with oxygen atoms. The reaction is self-accelerating and seems to engage different planes in a wave-like manner. Continuous field evaporation – the layer-by-layer removal in the presence of the imaging field – intervenes in carbon-free areas. The tip morphology developing progressively is very different from the one present before starting any experiment with reactive gases. The central (1 1 1) pole is small in Fig. 9e and f and surrounded by a triplet of small planes lying along <1 0 0> zones each. This specific structure (see Fig. 1a for comparison) needs further investigation in the future since we presently cannot exclude that a surface oxide is being formed and accompanied by a field-induced build-up [36].

Removing the oxygen from the gas mixture causes Fig. 9a to reappear in a short period of time. We mention that during this transition strong structural changes are observed to occur around the (1 1 1) pole: the number of layer edges increases dramatically and there is no doubt that this reconstruction must be attributed to ethylene adsorption/decomposition and carbide formation. Titration with oxygen as described above can be easily reproduced once the low-contrast micrograph of Fig. 9a is established. We note, however, that the layer edges of each of the symmetry-equivalent {1 1 0} planes may be equally acting as nucleation centre of the titration. Yet only one {1 1 0} plane at a time seems to be active and initiating the wave-like spread of the reaction. The detailed kinetics of the phenomenon will be addressed elsewhere.

It remains to be discussed why Ni tips containing carbon appear dim while those that turn metallic (or maybe oxygen-covered) appear bright. In the simple one-electron picture of field ionisation, the critical distance for field ionisation, $x_c = (I - \Phi)/eF$, increases with decreasing values of the work function (I, ionisation potential of the imaging species; F, electric field strength). Consequently, the field ionisation probability above such a surface is low. Independent measurements by Paolucci et al. [37] and Papagno et al. [38] have indeed demonstrated negative work function changes upon carbon chemisorption indicating a reversal of the surface dipole by accumulation of carbon in the subsurface region [39]. Quite similarly and in accordance with the above field ionisation model, we assume that the dim image in Fig. 9a is caused by the low ionisation probability above a carbidic, low-Φ Ni surface.

The occurrence of rather strong Ni–C bonds most probably contributes to the reluctance of the surface to undergo field evaporation. We note, however, that there is no simple relation between the evaporation field strength and the bond strength [7].

4. Conclusions

The results of PFDMS research presented here in some examples might help realizing the power of the methodical approach to studying kinetic reaction processes in adsorbed layers. Very few, if any, techniques are available to obtain such detailed insight into the mechanistic pathways of chemical reactions with a lateral resolution on the nanoscale. There is no doubt that the transformation of neutral surface species into field-desorbing ions presents a complicated process for itself. However, well-designed experiments as well as theoretical calculations can help characterizing and understanding this transformation.

The fact that field emitter tips can be regarded as excellent models of single catalyst grains free of any ceramic-like support material adds another credit point to applications of the PFDMS technique in basic catalysis research. Clearly, the simultaneous presence of a large number of exposed planes and the occurrence of surface diffusion make kinetic data evaluation sometimes cumbersome. A careful plane-to-plane analysis using the probe-hole approach may be of considerable help in this respect. If, on the other hand, site-selective processes are involved, like Ni-subcarbonyl formation in kinks or CO dissociation in Co steps which are both slow as compared to adsorption, kinetic data is accessible with very limited influence of the actual probe-hole position.

Reaction-induced reshaping of catalysts along with local plane reconstructions is an important issue which can be straightforwardly addressed by FIM. Dynamic processes can be imaged using video-techniques, see the removal of carbon by oxygen on Ni, and the combination with PFDMS provides a unique tool to follow dynamically changing surface structures and reactive processes in adsorbed layers along with local chemical compositions.

Acknowledgements

MM (research fellow) and TV (postdoctoral researcher) gratefully thank the Fonds de la Recherche Scientifique—FNRS for financial support. This work was also supported by the ‘‘Communauté Française de Belgique’’ (ARC, No. 96/01-201) which is also acknowledged.

References

[1] C.O. Bennett, Adv. Catal. 44 (1999) 329.
[2] P.L. Gai, E.D. Boyes, in: P.L. Gai (Ed.), In Situ Microscopy in Materials Research, Kluwer, Boston, 1997.
[3] P.L. Hansen, J.B. Wagner, S. Helveg, J.R. Rostrup-Nielsen, B.S. Clausen, H. Topsøe, Science 295 (2002) 2053.
[4] P.L. Hansen, S. Helveg, A.K. Datye, Adv. Catal. 50 (2006) 77.
[5] J. Wintterlin, Adv. Catal. 45 (2000) 131.
[6] J.V. Lauritsen, F. Besenbacher, Adv. Catal. 50 (2006) 97.
[7] E.W. Müller, T.T. Tsong, Field Ion Microscopy—Principles and Applications, Elsevier, New York, 1969.
[8] V. Gorodetskii, W. Drachsel, J.H. Block, Catal. Lett. 19 (1993) 223.
[9] C. Voss, N. Kruse, Appl. Surf. Sci. 87/88 (1995) 127.
[10] N. Kruse, T. Visart de Bocarmé, in: G. Ertl, H. Knözinger, J. Weitkamp, F. Schüth (Eds.), Handbook of Heterogeneous Catalysis, Wiley-VCH, in press.
[11] J.H. Block, in: A.W. Czanderna (Ed.), Methods and Phenomena, vol. 1, Elsevier Science Publishing Company, Amsterdam, 1975, p. 379.
[12] N. Kruse, G. Abend, J.H. Block, J. Chem. Phys. 88 (2) (1988) 1307.
[13] A. Mittasch, Z. Phys. Chem. 40 (1902) 1.
[14] G. Heinicke, Z. Anorg. Allg. Chem. 324 (1963) 173.
[15] G. Heinicke, H. Harenz, Z. Phys. Chem. 240 (1969) 325.
[16] O. Knacke, G. Lossmann, Z. Phys. Chem. (NF) 53 (1967) 272.
[17] H. Trivin, L. Bonnetain, Compt. Rend. (Paris) C268 (1969) 564.
[18] A.Ya. Kipnis, N.V. Kul’kova, N.F. Mikhailova, Kinet. Katal. 17 (1976) 472.
[19] D.E. Milliams, J. Pritchard, K.W. Sykes, Proceedings of the 6th International Congress on Catalysis 1 (1977) 417.
[20] P. De Groot, M. Coulon, K. Dransfeld, Surf. Sci. 94 (1980) 204.
[21] G. Greiner, D. Menzel, J. Catal. 77 (1982) 382.
[22] W.N. Shen, J.A. Dumestic, G.C. Hill Jr., J. Catal. 68 (1981) 152.
[23] W.A. Schmidt, J.H. Block, K.A. Becker, Surf. Sci. 122 (1982) 409.
[24] L. Mond, C. Langer, F. Quinke, J. Chem. Soc. 57 (1890) 749.
[25] N. Kruse, G. Abend, W. Drachsel, J.H. Block, in: Proceedings of the Eighth International Congress on Catalysis, vol. III, Weinheim, (1984), p. 105.
[26] D.B. Liang, G. Abend, J.H. Block, N. Kruse, Surf. Sci. 126 (1983) 392.
[27] V. Medvedev, R. Börner, N. Kruse, Surf. Sci. Lett. 401 (1998) L371.
[28] J.L. Gland, R.W. McCabe, G.E. Mitchell, Surf. Sci. 127 (1983) L123.
[29] J.C. Tracy, J. Chem. Phys. 56 (1972) 2736.

[30] H. Schulz (Ed.), Fischer Tropsch catalysis—science and practice, Top. Catal. (1–4), Springer, Netherlands, 2003, , 174p.
[31] J. Wilson, C. De Groot, J. Phys. Chem. 99 (1995) 7860.
[32] G.A. Beitel, A. Laskov, H. Osterbeek, E.W. Kuipers, J. Phys. Chem. B 100 (1996) 12494.
[33] P. Sabatier, Nobel Prize Lecture, 1912.
[34] R.T. Vang, K. Honkola, S. Dahl, E.K. Vestergaard, J. Schnadt, E. Laegsgaard, B.S. Clausen, J.K. Nørskov, F. Besenbacher, Surf. Sci. 600 (2006) 66.
[35] H. Nakano, J. Ogawa, J. Nakamura, Surf. Sci. 514 (2002) 256.
[36] R. Gomer, Field Emission and Field Ionisation, Harvard University Press, 1961.
[37] G. Paolucci, R. Rosei, K.C. Prince, A.M. Bradshaw, Appl. Surf. Sci. 22/23 (1985) 582.
[38] L. Papagno, M. Conti, L.S. Caputi, J. Anderson, G.J. Lapeyre, Phys. Rev. B 44 (1991) 1904.
[39] C. Klink, I. Stengaard, F. Besenbacher, E. Laegsgaard, Surf. Sci. 360 (1996) 171.